ANNALS OF GEOPHYSICS, 67, 2, DM213, 2024; doi:10.4401/ag-9050
OPEN ACCESS

A new technique based on the eigenvalue of the curvature tensor for enhancing gravity data

Luan Thanh Pham[1]

(1) Faculty of Physics, University of Science, Vietnam National University, Hanoi, Vietnam

Article History: received November 25, 2023; accepted May 20, 2024

Abstract

Enhancement of the boundaries of geologic structures is one of the main goals in interpretation of gravity anomalies. A range of different algorithms based on field derivatives has been introduced to solve this problem. Among these algorithms, the curvature gravity gradient tensor and its modifications are widely used in enhancing gravity data. These algorithms, however, have some main limitations such as the estimated edges are not compatible with the actual edges or bringing false information. In this study, I introduce a new technique based on the eigenvalue of the curvature tensor. The robustness of the presented technique is exemplified using model studies and a real-world dataset of the Vredefort dome (South Africa). The model studies show that the proposed filter can provide more accurate results and avoid artifacts in the output map. The real application result shows a good correlation between the edges highlighted by the presented algorithm and ring structures in the dome.

Keywords: Edge detection; Gravity data; Eigenvalue; Curvature tensor; Vredefort dome

1. Introduction

The initial geophysical method adopted for oil and gas exploration was the gravity method, which remains critic al and indispensable in some exploration regions, despite being overshadowed by seismology [Nabighian et al., 2005; Pham and Prasad, 2023; Ekinci et al., 2020, 2023; Narayan et al., 2023a, b, c]. In mining applications, the gravity technique is used to determine subsurface structures and calculate ore reserves for some massive sulphide ore deposits [Nabighian et al., 2005]. Interpretation of gravity anomalies provides valuable information on the horizontal location of causative geological bodies [Ekinci and Yigitbas, 2015; Kumar et al., 2018; Saibi et al., 2019; Ganguli et al., 2019, 2024; Sahoo et al., 2022a, b; Sarkar et al., 2022; Ekka et al., 2022; Pham et al., 2022a, Ganguli and Pal 2023; Narayan et al., 2021, 2023d; Kamto et al., 2023; Alvandi et al., 2023; Aprina et al., 2024]. Numerous filters have been provided to map source edges, mainly based on gradients of gravity anomaly data [Cordell and Grauch, 1979; Roest et al., 1992; Wijns et al., 2005; Ekinci et al., 2013; Kafadar, 2022; Nasuti et al., 2018, 2019; Pham et al., 2020; 2022b, c; Dwivedi and Chamoli 2021; Prasad et al., 2022a, b; Alvandi et al., 2023; Pham, 2023, 2024a, b].

Evjen [1936] initially used the zero value of the gravity vertical derivative (VD) to extract the borders. The method is formulated as:

$$VD = \frac{\partial F}{\partial z}. \tag{1}$$

The use of the zero value of the gravity second vertical derivative (SVD) is another technique for edge detection [Nabighian et al., 2005; Pal et al., 2016; Narayan et al., 2016]. The SVD can be obtained in the space domain from the horizontal derivatives by using the Laplace formula [Gupta and Ramani, 1982]:

$$SVD = \frac{\partial^2 F}{\partial z^2} = -\frac{\partial^2 F}{\partial x^2} - \frac{\partial^2 F}{\partial y^2}. \tag{2}$$

The SVD enhances near-surface anomalies at the expense of deeper anomalies [Pal and Majumdar, 2015; Vaish and Pal, 2015]. However, the width of the SVD is narrower than the VD and thus supposedly easier to interpret [Mickus, 2021].

Miller and Singh [1994] introduced a normalized detector, called the tilt derivative (TDR), that is based on the ratio of derivatives of gravity data. The method uses the zero contours of the tilt derivative to extract the source edges, and is given by:

$$TDR = atan \frac{\frac{\partial F}{\partial z}}{\sqrt{\left(\frac{\partial F}{\partial x}\right)^2 + \left(\frac{\partial F}{\partial y}\right)^2}}. \tag{3}$$

Oruç et al. [2013] introduced the curvature gravity gradient tensor (CGGT) to determine horizontal locations of isolated bodies. The matrix is constructed from the tensor components of the gravity potential g, and is defined as:

$$\Gamma = \begin{pmatrix} g_{xx} & g_{xy} \\ g_{yx} & g_{yy} \end{pmatrix}. \tag{4}$$

The determinant of the curvature gradient matrix $\det(\Gamma)$ is used to map the borders of gravity data [Oruç et al., 2013], which is given by:

$$\det(\Gamma) = \lambda_1 \lambda_2, \tag{5}$$

where the eigenvalues λ of Γ are given by:

$$\lambda_1 = \frac{1}{2}\left(g_{xx} + g_{yy} + \sqrt{\left(g_{xx} - g_{yy}\right)^2 + 4g_{xy}^2}\right), \tag{6}$$

and

$$\lambda_2 = \frac{1}{2}\left(g_{xx} + g_{yy} - \sqrt{\left(g_{xx} - g_{yy}\right)^2 + 4g_{xy}^2}\right). \tag{7}$$

According to Zhou et al. [2013], the CGGT method cannot be applied to complex gravity datasets including both positive and negative data. They improved the CGGT method using a combination of the gravity anomaly with large eigenvalue (IE). Their method is given by [Zhou et al., 2013]:

$$IE = \frac{1}{2}\left(g_{xx} * F + g_{yy} * F + \sqrt{\left(g_{xx} * F - g_{yy} * F\right)^2 + 4\left(g_{xy} * F\right)^2}\right). \tag{8}$$

The zero contours of the $\det(\Gamma)$ and IE are used to outline the borders of causative geological bodies [Oruç et al., 2013; Zhou et al., 2013; Dung, 2016; Dung et al., 2019]. However, these methods produce false edges or the estimated edges are not in good agreement with the real edges [Zhou and Geng, 2014; Wang et al., 2015].

The goal of this work is to present a new technique based on the eigenvalue of the curvature tensor to map source edges with higher accuracy and without artifacts. I have demonstrated the application of the new technique on model studies and a real dataset of the Vredefort dome, South Africa.

2. New method

Similar to the curvature tensor of the gravity potential [Oruç et al., 2013], the curvature tensor of the gravity anomaly F is constructed from the tensor components of the gravity anomaly, and is defined by:

$$\Gamma^F = \begin{pmatrix} F_{xx} & F_{xy} \\ F_{yx} & F_{yy} \end{pmatrix}. \tag{9}$$

The eigenvalues λ of the matrix are given by:

$$\lambda_1^F = \frac{1}{2}\left(F_{xx} + F_{yy} + \sqrt{\left(F_{xx} - F_{yy}\right)^2 + 4F_{xy}^2}\right), \tag{10}$$

and

$$\lambda_2^F = \frac{1}{2}\left(F_{xx} + F_{yy} - \sqrt{\left(F_{xx} - F_{yy}\right)^2 + 4F_{xy}^2}\right). \tag{11}$$

Here, I follow Zhou et al. [2013] to create a new filter by combining the gravity anomaly with large eigenvalue (GE), which is defined as:

$$GE = \frac{1}{2}\left(F_{xx} * F + F_{yy} * F + \sqrt{\left(F_{xx} * F' - F_{yy} * F'\right)^2 + 4\left(F_{xy} * F'\right)^2}\right), \tag{12}$$

where F' is obtained by multiplying the field F by a positive constant less than one k. In general, $k = \dfrac{|F_{max}|}{|F_{min}| + |F_{max}|}$ will yield the best result, however, in some cases, the value of k should be decided from the result.

The primary goal of the suggested technique is to identify locations with sudden variations in density. Similar to the IE technique, the zero contours of the GE present the borders of the bodies. Since the proposed filter does not use the vertical derivatives, it is less sensitive to noise than the recent techniques.

In this study, the suggested technique and others are implemented in Matlab programming language environment.

3. Synthetic tests

In this section, I examine the validity of the present filter on two synthetic models. I also compare the outputs of my filter with those calculated by other filters such as VD, SVD, TDR, CGGT and IE.

The first model includes three prismatic sources A1, A2 and A3 with positive density contrasts. Parameters of the sources are given in Table 1. The 3D view and theoretical gravity anomaly of the model are depicted in Figs. 1a and 1b, respectively. Figs. 2a-2f present the VD, SVD, TDR, CGGT, IE and GE filters of the anomaly in Fig. 1b, respectively. The zero contours of these filters are shown by the red lines, while the dashed green lines show the true edges. As depicted in these figures, the VD and TDR cannot discriminate between three prismatic sources,

and present them as if they are resulted from one body (Figs. 2a and 2c). The CGGT and IE provide a more precise estimation of the borders than the VD and TDR, but the CGGT brings other additional edges, while the IE method does not (Figs. 2d and 2e). In addition, the edges of the sources A2 and A3 are significantly deformed. Although, both the SVD and GE have a better performance in mapping the edges compared to other filters, the zero contours in the SVD map are shifted outward from the real edge locations of the deeper sources A2 and A3 (Figs. 2b and 2f). Comparing Figs. 2a-2f shows that the GE filter gives the most accurate estimation of the source edges.

Parameters	A1	A2	A3
Center coordinates (km; km)	2; 2.4	1.55; 1.7	2.45; 1.7
Width (km)	0.3	0.4	0.5
Length (km)	0.3	0.4	0.5
Depth to the top (km)	0.1	0.25	0.4
Depth to the bottom (km)	0.4	0.6	0.8
Density contrast (g/cm^3)	0.1	0.25	0.3

Table 1. Parameters of the first model.

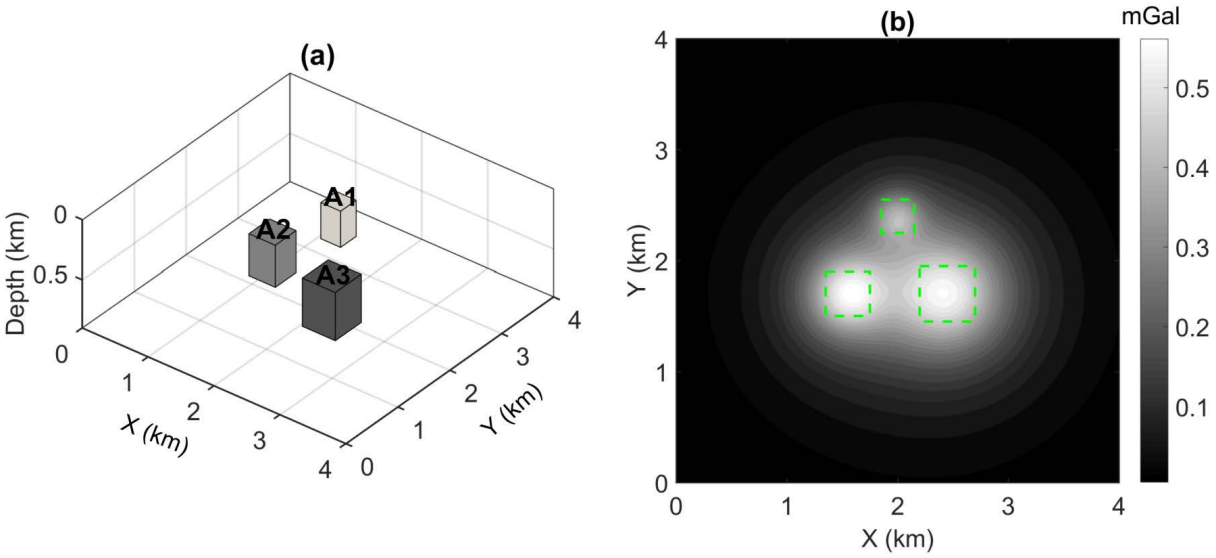

Figure 1. (a) The first model, (b) Gravity anomaly of the sources with positive density contrasts. The green lines indicate the real borders of the sources.

The second one includes four larger prismatic sources B1, B2, B3 and B4, which is similar to the model of Oruç et al. [2013]. The model includes both positive and negative density contrasts with parameters given in Table 2. The 3D view of the model and its gravity data are depicted in Fig. 3a and 3b, respectively. Figures 4a-4f show the VD, SVD, TDR, CGGT, IE and GE filters of data of Figure 3b, respectively. It can be seen that the VD and TDR generate false edges (Figs. 4a and 4c). These filters cannot map the western edge of the body B3 (Figs. 4a and 4c). In addition, the estimated edges of the deep sources (B2, B3 and B4) show the bodies larger than reality (Figs. 4a and 4c). Although the SVD shows a better result compared with the VD and TDR, it still brings false edge information (Fig. 4b). It can

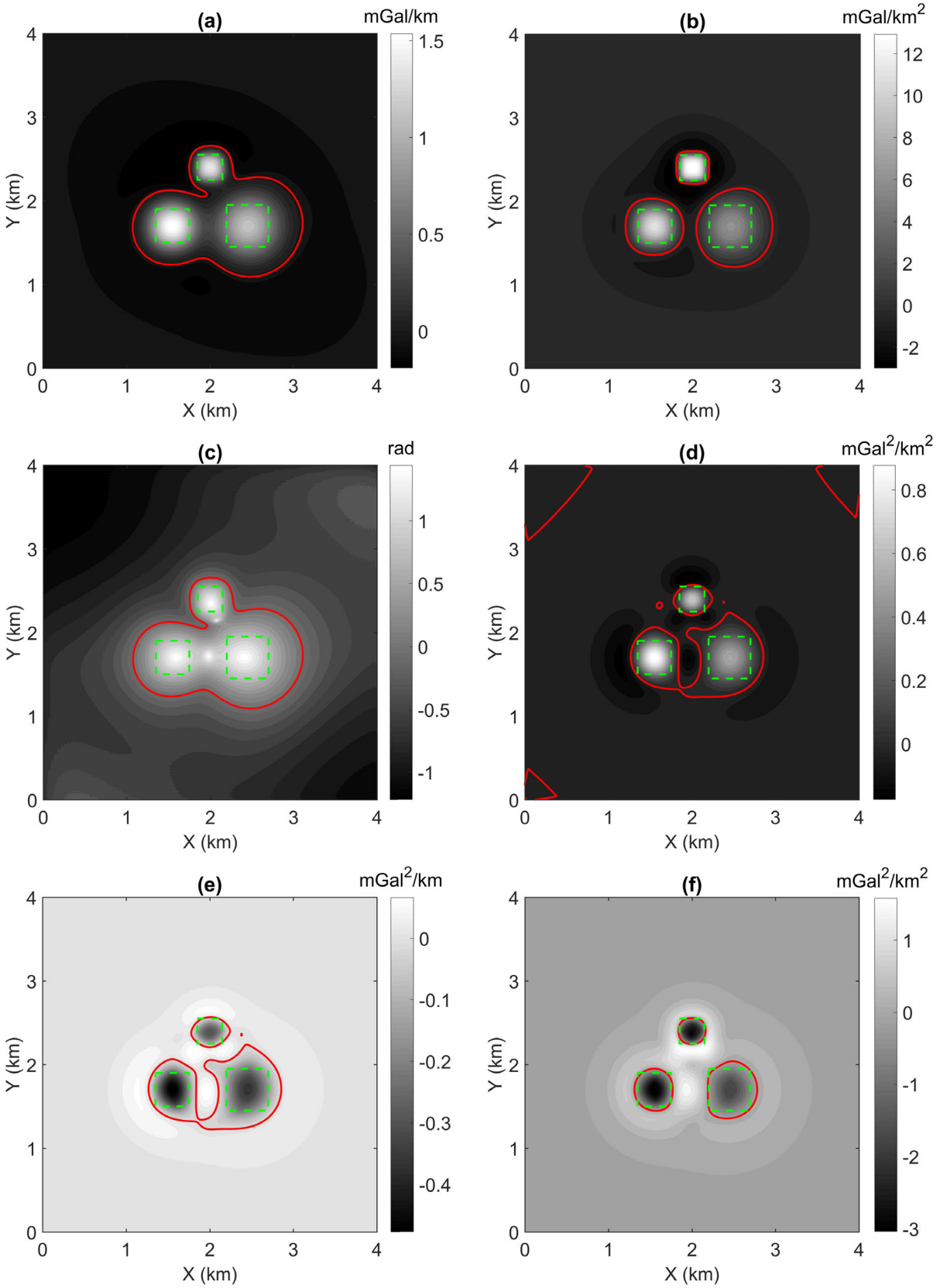

Figure 2. Enhancement of gravity data of the first model with positive density contrasts: (a) VD, (b) SVD, (c) TDR, (d) CGGT, (e) IE, (f) GE. The green lines indicate the real borders of the sources, and the red lines are zero contours.

be seen from Fig. 4d that the CGGT allows for a more precise estimate of the borders than the VD, SVD and TDR, but it generates some small artificial structures. In this case, the IE and GE can map all the borders without other additional borders (Figs. 4e and 4f). However, the zero contours in the IE map are shifted outward from the true borders of the deep prisms B2, B3 and B4 (Fig. 4e). According to these findings, I can say that the GE technique provides better performance in boundary mapping compared with the VD, SVD, TDR, CGGT and IE filters.

Parameters	B1	B2	B3	B4
Center coordinates (km; km)	12.5; 34	33; 39	32; 23	15; 12.5
Width (km)	5	7	15	10
Length (km)	22	7	8	5
Depth to the top (km)	0.5	1.5	2	1
Depth to the bottom (km)	10	10	10	10
Density contrast (g/cm^3)	0.2	−0.2	−0.2	0.2

Table 2. Parameters of the second model.

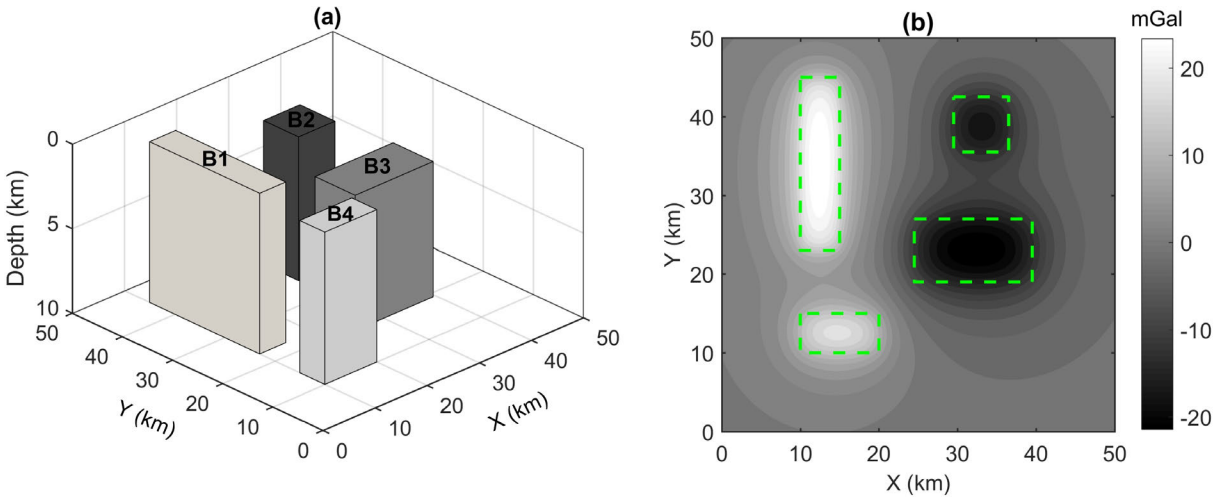

Figure 3. (a) The second model, (b) Gravity anomaly of the sources with positive and negative density contrasts. The green lines indicate the real borders of the sources.

To delve deeper into the ability of the proposed filter to identify source edges in the presence of noise, I added Gaussian noise with an amplitude of 0.2% of the anomaly amplitude to the observed field (Fig. 5a). Figures 5b-5g show the VD, SVD, TDR, CGGT, IE and GE filters of anomalies in Figure 5a, respectively. One can see from these figures, the VD, SVD, TDR and GE filters are more noise-sensitive than the CGGT and IE methods. The reason is that the VD, SVD, TDR and GE filters use the vertical derivative or second order horizontal derivatives of the gravity anomaly, while the CGGT and IE use second order horizontal derivatives of the gravity potential. Although the CGGT and IE are less sensitive to noise, the bodies estimated from these techniques appear larger than their actual size. For the noisy field, it is advised to apply an upward continuation filter to eliminate noise before calculating the

borders [Nasuti and Nasuti, 2018]. Figure 5h depicts the GE result after applying a 1 km upward continuation filter. As can be seen from this map, the proposed technique GE can provide a more accurate estimate of the anomaly borders even though the field is affected by the upward continuation filter.

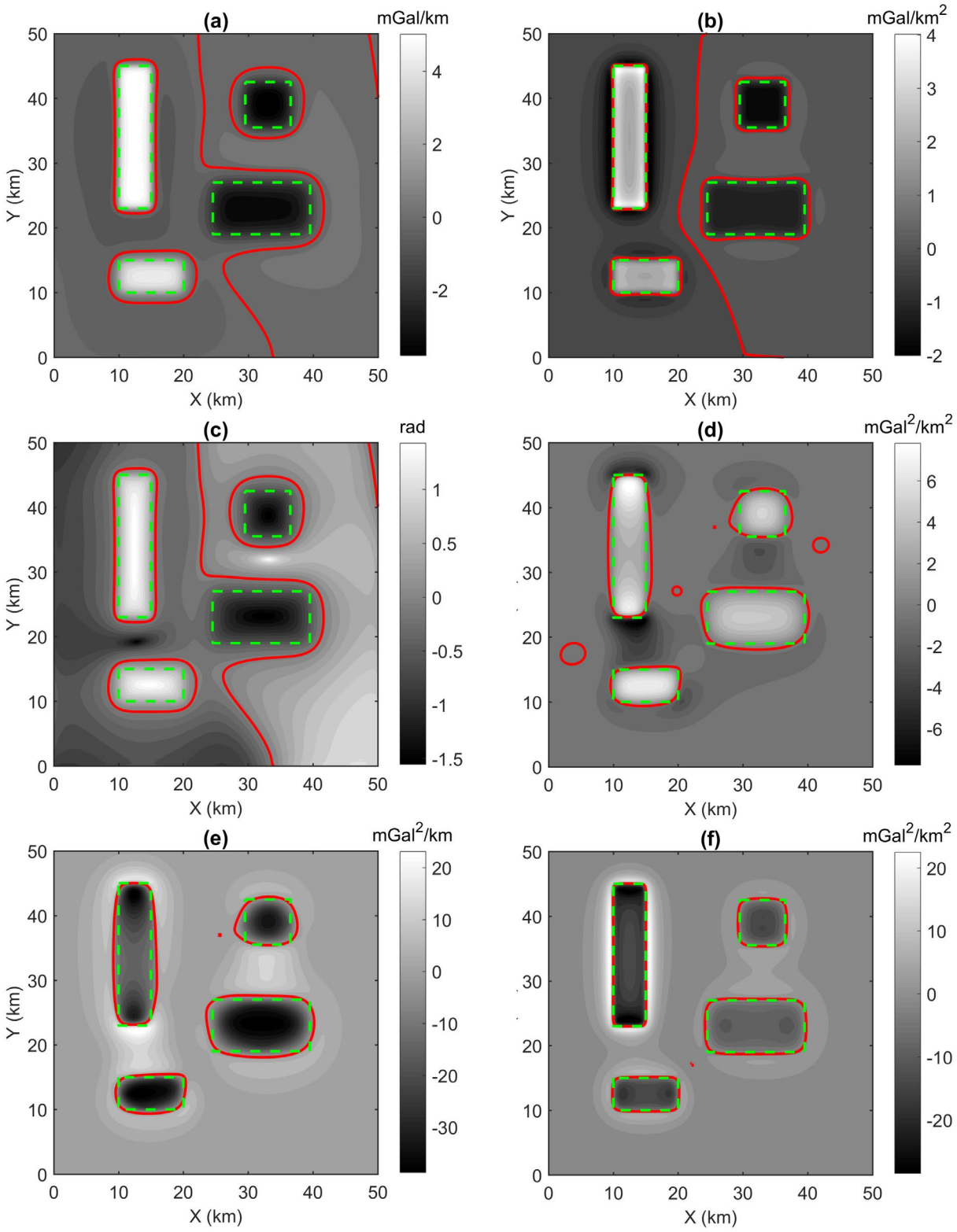

Figure 4. Enhancement of gravity data of the second model with positive and negative density contrasts: (a) VD, (b) SVD, (c) TDR, (d) CGGT, (e) IE, (f) GE. The green lines indicate the real borders of the sources, and the red lines are zero contours.

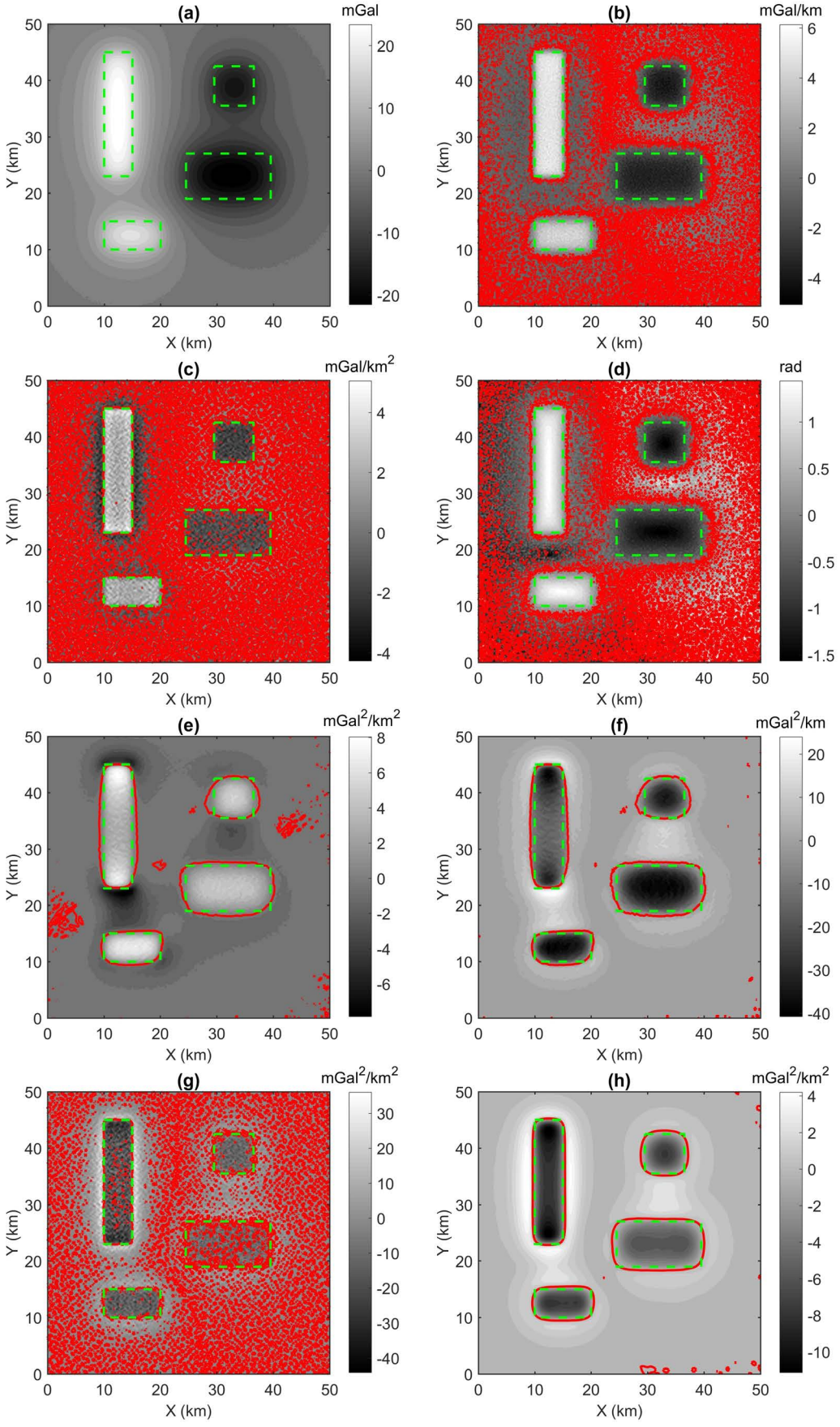

Figure 5. (a) Gravity data in Figure 3b contaminated with Gaussian noise having an amplitude of 0.2% of the anomaly amplitude, (b) VD, (c) SVD, (d) TDR, (e) CGGT, (f) IE, (g) GE of noisy data in Figure 5a, (h) GE of 1 km upward-continued data. The green lines indicate the real borders of the sources, and the red lines are zero contours.

4. Real study

The practical application of the new filter GE was estimated by outlining structural features of the Vredefort dome. The dome is located in the Witwatersrand Basin, South Africa (Fig. 6). It is the largest verified impact structure on Earth [Jahn and Riller, 2009]. The dome includes a 40 km wide core of high-grade Archean gneisses that is surrounded by a 15-20 km wide collar of late Archaean to early Proterozoic rocks (Fig. 6) [Lana et al., 2003; Dellefant et al., 2022]. The Archean basement rocks in this core are composed of a complex high-grade metamorphic terrane that is dominated by gneisses (Fig. 6). The southern and southeastern parts are largely obscured by Phanerozoic sediments (Fig. 6).

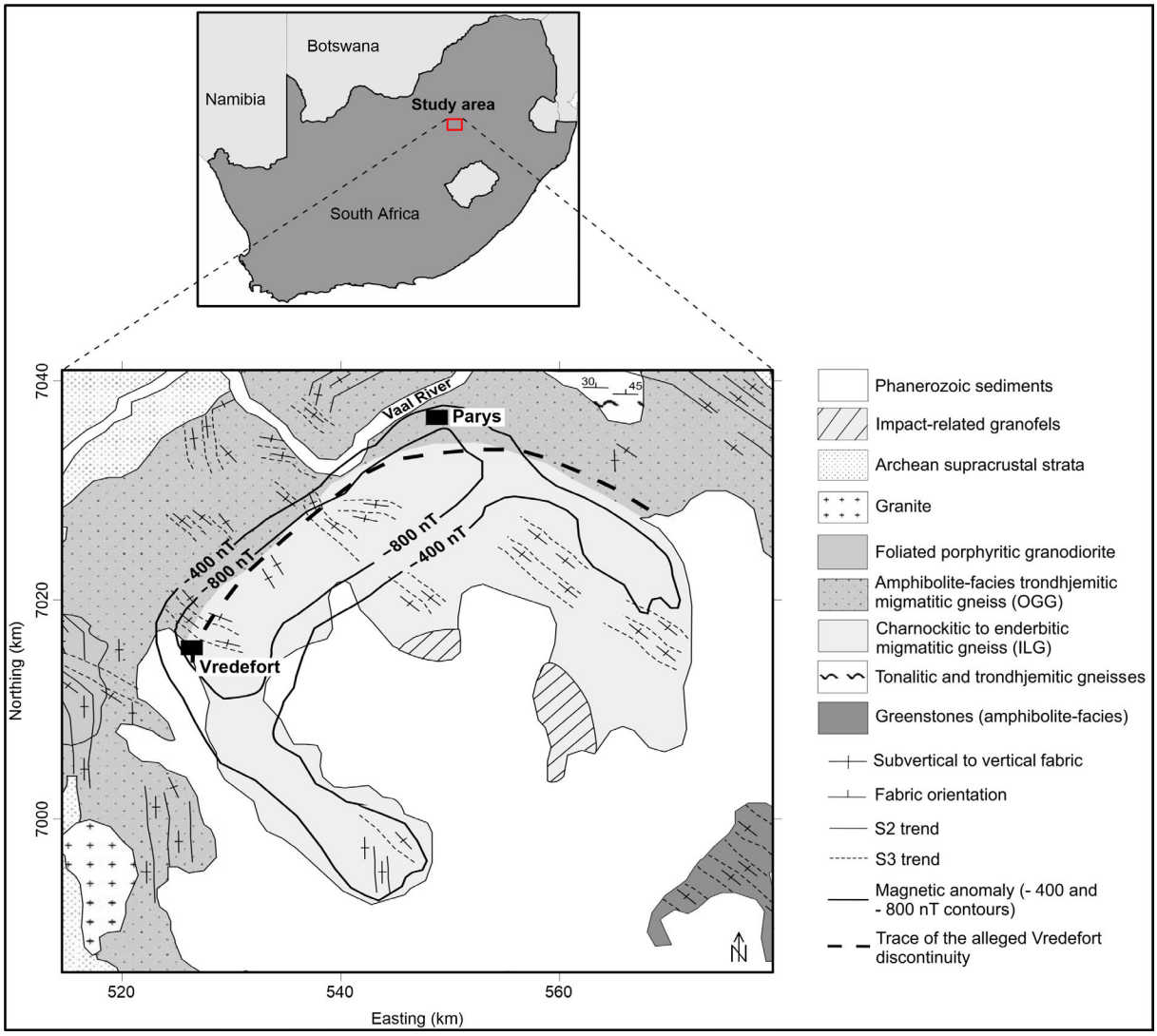

Figure 6. Geological map of the Vredefort dome [modified from Lana et al., 2003].

The Bouguer gravity anomalies of the area was provided by the Council for Geoscience, South Africa. The Bouguer gravity map is shown in Figure 7 with 1 km grid spacing.

Figures 8a-8c show the VD, SVD and TDR of anomalies in Figure 7, respectively. As can be seen, the findings obtained from these techniques are quite similar. However, the SVD map provides more structural features than the VD and TDR. Figs. 8d-8e show the CGGT and IE of anomalies in Figure 7, respectively. As presented in these figures, the CGGT brings a complicated map of structural features, while the boundaries in the IE map are discontinuous. The result of the presented method is shown in Fig. 8f. This result demonstrates the existence of ring structures in

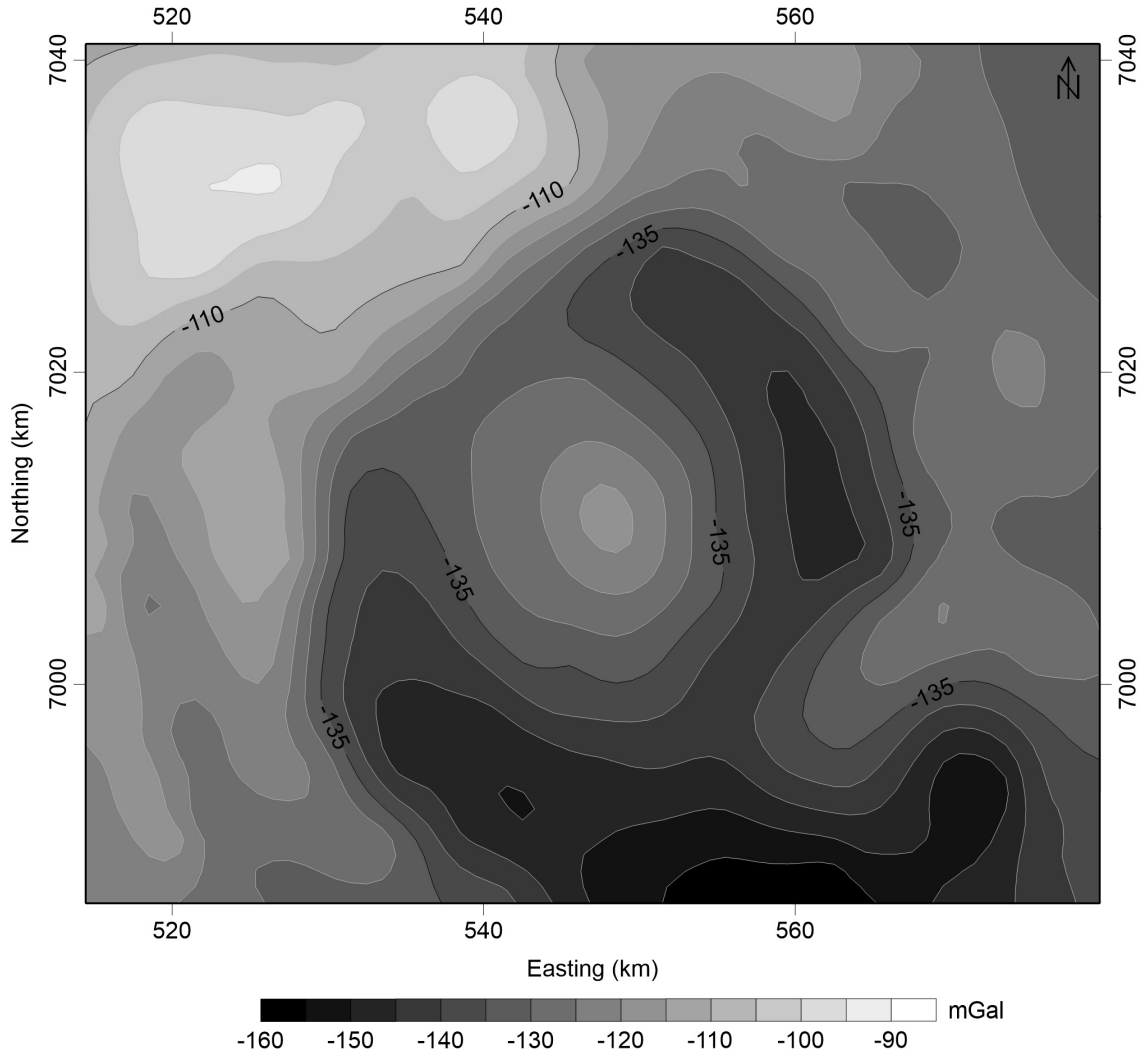

Figure 7. Bouguer gravity anomaly of the Vredefort dome.

the dome, as reported by some other authors [e.g., Beiki, 2010; Beiki and Pedersen, 2010; Pham et al., 2021]. These structures are well correlated with the geological map of the dome. In addition, the CGGT, IE, and GE maps revealed the presence of an isolated body beneath sediments in the southeastern corner of the dome. The result in the CGGT map shows some additional boundaries that are not represented in the IE and GE maps. However, these boundaries may be false edges that appeared in the theoretical examples. Although the VD, SVD and TDR and GE demonstrate the existence of ring structures in the dome, the GE result shows smaller causative geological bodies than those from the VD, SVD and TDR. As demonstrated in the theoretical examples, the GE has lower source depth sensitivity, while the VD, SVD and TDR results bring the structure larger than its true size for the deep sources. Therefore, it can say that the result obtained from the proposed technique GE provides a more precise estimate of the borders of the geological bodies in the Vredefort dome.

5. Conclusions

I have introduced a new filter (GE) for more precisely mapping the source borders. The presented filter was demonstrated on synthetic examples, and gravity anomalies from the Vredefort dome, South Africa. The GE filter is able to map the borders of gravity data with more accuracy and without spurious edges when compared to other filters. Further, as a real data application, the estimated boundaries from anomalies of the Vredefort dome demonstrate the existence of ring structures in the dome. Consequently, I conclude that the presented technique is a useful tool for outlining the source borders from gravity anomalies.

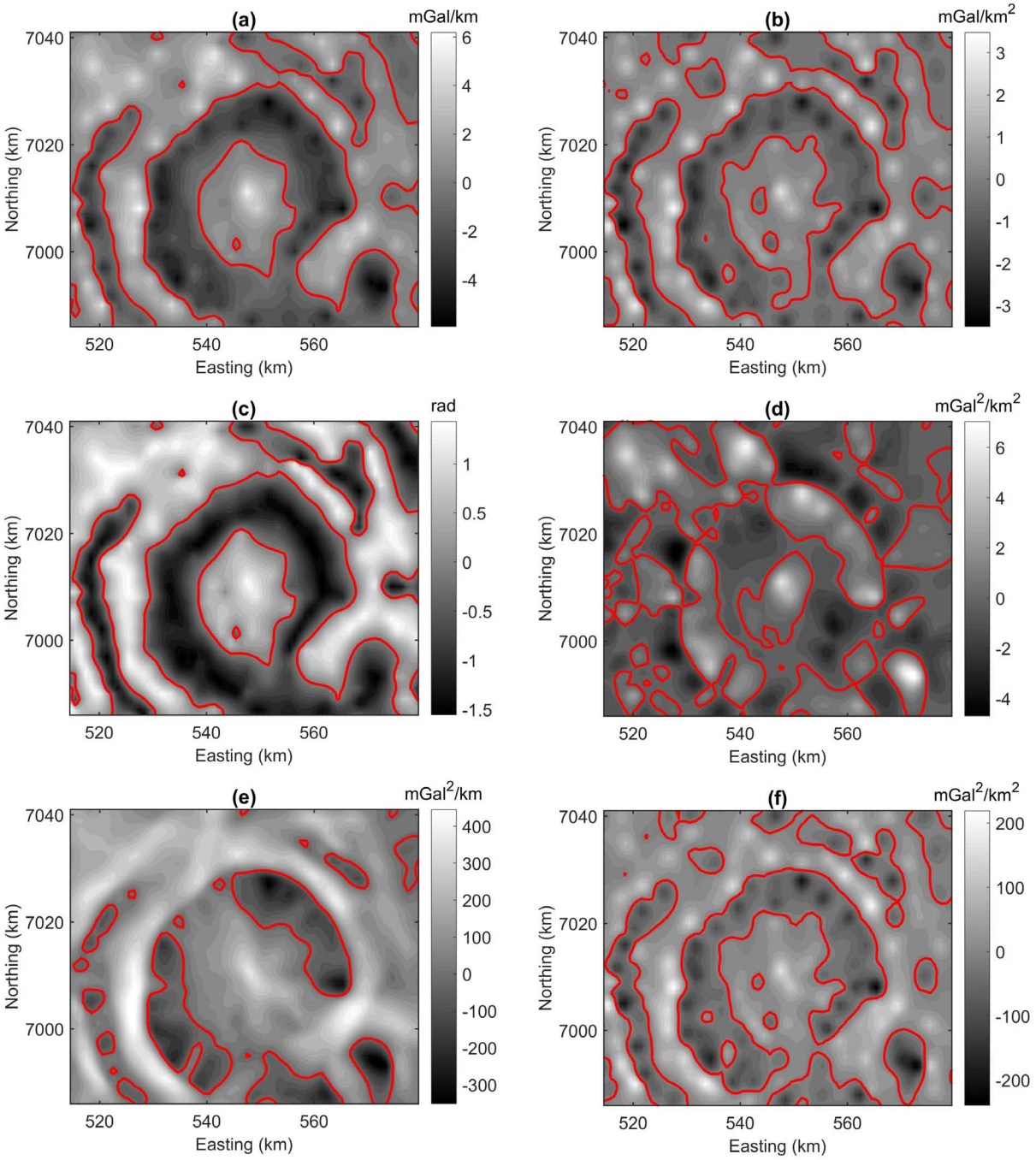

Figure 8. (a) VD, (b) SVD, (c) TDR, (d) CGGT, (e) IE, (f) GE. The red lines show zero contours.

References

Alvandi, A., K. Su, H. Ai, V.E. Ardestani and C. Lyu (2023). Enhancement of potential field source boundaries using the hyperbolic domain (Gudermannian function), Minerals, 13, 10, 1312.

Aprina, P.U., D. Santoso, S. Alawiyah, N. Prasetyo, K. Ibrahim (2024). Delineating geological structure utilizing integration of remote sensing and gravity data: a study from Halmahera, North Molucca, Indonesia, Vietnam J. Earth Sci., 46, 2, 147-168.

Cordell, L. and V.J.S. Grauch (1985). Mapping basement magnetization zones from aeromagnetic data in the San Juan Basin, New Mexico, in The Utility of Regional Gravity and Magnetic Maps, 1st edn, 181-197, ed. Hinze, W.J., Society of Exploration Geophysicists.

Beiki, M. and L.B. Pedersen (2010). Interpretation of gravity gradient tensor data using eigenvector analysis: An example from the Vredefort impact structure, South Africa, SEG Technical Program Expanded Abstracts, 1146-1151.

Beiki, M. (2010) Analytic signals of gravity gradient tensor and their application to estimate source location, Geophysics, 75, 6, I59- I74.

Dellefant, F., C.A. Trepmann, S.A. Gilder, I.V. Sleptsova, M. Kaliwod and B.P. Weiss (2022). Ilmenite and magnetite microfabrics in shocked gneisses from the Vredefort impact structure, South Africa. Contrib. Mineral Petrol., 177, 88.

Dung, N.K. (2016) Application of the new method to determine the main structure of the Pre-Cenozoic basement in the Gulf of Tonkin and adjacent area. Vietnam Journal of Marine Science and Technology, 16(4), 356-363.

Dung, N.K., D.D. Thanh, H.V. Vuong and D.T.H. Thu (2019) Using the combination of the 3d gravity inversion method with the directional analytic signal derivatives and the curvature gravity gradient tensor method to determine structure of the Pre-cenozoic basement on southeast continental shelf of Vietnam. Vietnam Journal of Marine Science and Technology, 18(4), 393-405.

Dwivedi, D. and A. Chamoli (2021) Source edge detection of potential field data using wavelet decomposition. Pure Appl. Geophys., 178 (3), 919-938.

Ekka, M.S., S.D. Sahoo, S.K. Pal, P.N. Singha Roy and O.P. Mishra (2022). Comparative analysis of the structural pattern over the Indian Ocean basins using EIGEN6C4 Bouguer gravity data, Geocarto Int., 37, 26, 14198-14226.

Ekinci, Y.L.C., E. Ertekin and E. Yigitbas (2013). On the effectiveness of directional derivative based filters on gravity anomalies for source edge approximation: synthetic simulations and a case study from the Aegean graben system (western Anatolia, Turkey). J. Geophys. Eng., 10, 3, 035005.

Ekinci, Y.L. and E. Yigitbas (2015). Interpretation of gravity anomalies to delineate some structural features of Biga and Gelibolu peninsulas, and their surroundings (north-west Turkey), Geodinam Acta., 27, 4, 300-319.

Ekinci, Y.L., C. Balkaya, G. Göktürkler and Ş. Özyalın (2020). Gravity data inversion for the basement relief delineation through global optimization: a case study from the Aegean Graben System, western Anatolia, Turkey, Geophys. J. Int. 224, 2, 923-944.

Ekinci, Y.L., C. Balkaya, G. Göktürkler and H. Ai (2023). 3-D gravity inversion for the basement relief reconstruction through modified success-history-based adaptive differential evolution, Geophys. J. Int., 235, 1, 377-400.

Evjen, H.M (1936). The place of the vertical gradient in gravitational interpretations, Geophys., 1, 1, 127-136.

Ganguli, S.S., S. Singh, N. Das, D. Maurya, S.K. Pal and J.V. Rama Rao (2019). Gravity and Magnetic Survey in Southwestern Part of Cuddapah Basin, India and its Implication for Shallow Crustal Architecture and Mineralization, J. Geol. Soc. India, 93, 419-430.

Ganguli, S.S. and S.K. Pal (2023). Gravity-magnetic appraisal of the southern part of the Cauvery Basin, Eastern Continental Margin of India (ECMI): evidence of a volcanic rifted margin, Front. Earth Sci., 11, 1190106.

Ganguli, S.S., S. Kumar and R.K. Singh (2024) Crustal architecture of the Dharwar craton and Southern Granulite Terrane, Southern India, from the analysis of gravity-magnetic data, Phys. Chem. Earth, Parts, A/B/C, 133, 103532.

Gupta, V.K. and N. Ramani (1982). Optimum second vertical derivatives in geologic mapping and mineral exploration, Geophys., 47, 12, 1706-1715.

Jahn, A. and U. Riller (2009). A 3D model of first-order structural elements of the Vredefort Dome, South Africa – importance for understanding central uplift formation of large impact structures, Tectonophys., 478, 3-4, 221-229.

Kafadar, O. (2022). Applications of the Kuwahara and Gaussian filters on potential field data, J. Appl. Geophys., 198, 104583.

Kamto, P.G., E. Oksum, L.T. Pham and J. Kamguia (2023). Contribution of advanced edge detection filters for the structural mapping of the Douala Sedimentary Basin along the Gulf of Guinea, Vietnam J. Earth Sci., 45, 3, 287-302.

Kumar, U., S.K. Pal, S.D. Sahoo, S. Narayan, S. Saurabh Mondal and S.S. Ganguli (2018). Lineament mapping over Sir Creek offshore and its surroundings using high resolution EGM2008 Gravity data: an integrated derivative approach, J. Geol. Soc. India., 91, 671-678.

Lana, C., R.L. Gibson, A.F.M. Kisters and W.U. Reimold (2003) Archean crustal structure of the Kaapvaal craton, SouthAfrica – evidence from the Vredefort dome, Earth Planet. Sci. Lett., 206, 133-144.

Mickus, K. (2021). Geophysical methods, in Pollution Assessment for Sustainable Practices in Applied Sciences and Engineering, 199-287, ed. Mohamed, A.M.O., E.K. Paleologos and F.M. Howari. https://doi.org/10.1016/B978-0-12-809582-9.00005-0.

Miller, H.G. and V. Singh (1994). Potential field tilt—a new concept for location of potential field sources, J. Appl. Geophys., 32(2-3), 213-217.

Nabighian, M.N., M.E. Ander, V.J.S. Grauch, R.O. Hansen, T.R. LaFehr, Y. Li, et al. 2005. Historical development of the gravity method in exploration, Geophys., 70, 6, 63-89.

Narayan, S., S.D. Sahoo, S.K. Pal, U. Kumar, V.K. Pathak, T.J. Majumdar and A. Chouhan (2016). Delineation of structural features over a part of the Bay of Bengal using total and balanced horizontal derivative techniques, Geocarto Int., 32, 4, 351-366.

Narayan, S., U. Kumar, S.K. Pal and S.D. Sahoo (2021). New insights into the structural and tectonic settings of the Bay of Bengal using high-resolution earth gravity model data, Acta Geophys., 69, 2011-2033.

Narayan, S., S.D. Sahoo, S.K. Pal, L.T. Pham and P. Kumar (2023a). Integrated geophysical and petrophysical characterization of Upper Jurassic carbonate reservoirs from Penobscot field, Nova Scotia: a case study, Mar. Geophys. Res., 44, 23 (2023), https://doi.org/10.1007/s11001-023-09533-0.

Narayan, S., R. Singh, A. Mohan, K. Vivek, P. Acharya and S.K. Pal (2023b). Delineation of thin and discrete sand reservoir facies from shale-dominated Kopili Formation (Middle to Late Eocene) using the post-stack seismic inversion and neural network algorithm: A case study from Assam Basin, India. J. Earth Syst. Sci., 132, 81.

Narayan, S., S.D. Sahoo, S. Kar, S.K. Pal and S. Kangsabanik (2023c) Improved reservoir characterization by means of supervised machine learning and model-based seismic impedance inversion in the Penobscot field, Scotian Basin, Energy Geoscience, 100180 https://doi.org/10.1016/j.engeos.2023.100180.

Narayan, S., S.D. Sahoo, S.K. Pal and U. Kumar (2023d). Comparative evaluation of five global gravity models over a part of the Bay of Bengal, Adv. Space Res., 71, 5, 2416-2436.

Nasuti, Y. and A. Nasuti (2018). NTilt as an improved enhanced tilt derivative filter for edge detection of potential field anomalies, Geophys. J. Int., 214, 1, 36-45.

Nasuti, Y., A. Nasuti and D. Moghadas (2019). STDR: A novel approach for enhancing and edge detection of potential field data. Pure Appl. Geophys., 176, 2, 827-841.

Oruç, B., I. Sertcelik, O. Kafadar and H.H. Selim (2013). Structural interpretation of the Erzurum Basin, eastern Turkey, using curvature gravity gradient tensor and gravity inversion of basement relief, J. Appl. Geophys., 88, 105-113.

Pal, S.K. and T.J. Majumdar (2015). Geological appraisal over the Singhbhum-Orissa Craton, India using GOCE, EIGEN6-C2 and in situ gravity data, Int. J. Appl. Earth Obs. Geoinfo., 35, 96-119.

Pal, S.K., S. Narayan, T.J. Majumdar and U. Kumar (2016) Structural mapping over the 85°E Ridge and surroundings using EIGEN6C4 high-resolution global combined gravity field model: an integrated approach, Marine Geophys. Res., 37, 3, 159-184.

Pham, L.T. (2023). A novel approach for enhancing potential fields: application to aeromagnetic data of the Tuangiao, Vietnam. Eur. Phys. J. Plus, 138, 12, 1134.

Pham, L.T. (2024a). An improved edge detector for interpreting potential field data, Earth Sci. Inform., 17, 2763-2774.

Pham, L.T. (2024b). A stable method for detecting the edges of potential field sources, IEEE Trans. Geosci. Remote Sens., 62:5912107.

Pham, L.T., T.V. Vu, S. Le-Thi and P.T. Trinh (2020). Enhancement of potential field source boundaries using an improved logistic filter, Pure Appl. Geophys., 177, 5237-5249.

Pham, L.T., E. Oksum, O. Kafadar, P.T. Trinh, D.V. Nguyen, Q.T. Vo, S.T. Le and T.D. Do (2022a) Determination of subsurface lineaments in the Hoang Sa islands using enhanced methods of gravity total horizontal gradient, Vietnam J. Earth Sci., 44, 3, 395-409.

Pham, L.T., A.M. Eldosouky, E. Oksum and S.A. Saada (2022b). A new high resolution filter for source edge detection of potential field data. Geocarto Int., 37, 11, 3051-3068.

Pham, L.T., E. Oksum, D.V. Le, F.J.F. Ferreira and S.T. Le (2022c). Edge detection of potential field sources using the softsign function. Geocarto Int., 3, 14, 4255-4268.

Pham, L.T. and K.N.D. Prasad (2023) Analysis of gravity data for extracting structural features of the northern region of the Central Indian Ridge, Vietnam J. Earth Sci., 45, 2, 147-163.

Prasad, K.N.D., L.T. Pham and A.P. Singh (2022a). A novel filter "ImpTAHG" for edge detection and a case study from Cambay Rift Basin, India, Pure Appl Geophys., 179, 6-7, 2351-2364.

Prasad, K.N.D., L.T. Pham and A.P. Singh (2022b). Structural mapping of potential field sources using BHG filter, Geocarto Int., 37, 26, 11253-11280.

Roest, W.R., J. Verhoef and M. Pilkington (1992) Magnetic interpretation using the 3-D analytic signal, Geophys., 57, 1, 116-125.

Sahoo, S.D., S.K. Narayan and S.K. Pal (2022a). Fractal analysis of lineaments using CryoSat-2 and Jason-1 satellite-derived gravity data: Evidence of a uniform tectonic activity over the middle part of the Central Indian Ridge, Phys Chem Earth, Parts A/B/C 128:103237.

Sahoo, S., S. Narayan and S.K. Pal (2022b) Appraisal of gravity-based lineaments around Central Indian Ridge (CIR) in different geological periods: Evidence of frequent ridge jumps in the southern block of CI,. J. Asian Earth Sci. 239, 105393.

Saibi, H., G. Amir and F.S. Mohamed (2019). Subsurface structural mapping using gravity data of AlAin region, Abu Dhabi Emirate, United Arab Emirates. Geophys J Int., 216, 2, 1201-1213.

Sarkar, P., S. Mondal, S.K. Pal, P.N.S. Roy, S.D. Sahoo, A. Widyadwatmaja, S. Gupta and A. Gupta (2022) New insights on the tectonic framework using EIGEN6C4 gravity data, seismicity, and finite element stress analysis: an attempt to map earthquake vulnerable zones in parts of North-East India and surroundings, Phys Chem Earth, 127, 103195.

Vaish, J. and S.K. Pal (2015). Geological mapping of Jharia Coalfield, India using GRACE EGM2008 gravity data: a vertical derivative approach, Geocarto Int., 30, 4, 388-401, doi:10.1080/10106049.2014.905637.

Wang, J., X. Meng and F. Li (2015). Improved curvature gravity gradient tensor with principal component analysis and its application in edge detection of gravity data, J. Appl. Geophys., 118, 106-114.

Wijns, C., C. Perez and P. Kowalczyk (2005). Theta map: Edge detection in magnetic data, Geophys., 70, 4, L39-43.

Wilton, D.H.C., G.M. Thompson and D. Evans-Lamswood (2021). MLA-SEM Characterization of Sulphide Weathering, Erosion, and Transport at the Voisey's Bay Orthomagmatic Ni-Cu-Co Sulphide Mineralization, Labrador, Canada, Minerals., 11, 1224.

Zhou, W.N., X.J. Du and J.Y. Li (2013). The limitation of curvature gravity gradient tensor for edge detection and a method for overcoming it, J. Appl. Geophys., 98, 237-242.

Zhou, S. and M. Geng (2014) Comment on "Structural interpretation of the Erzurum Basin, eastern Turkey, using curvature gravity gradient tensor and gravity inversion of basement relief" by B. Oruç et al. (2013), J. Appl. Geophys., 111, 393-394.

***CORRESPONDING AUTHOR: Luan Thanh PHAM**,
Faculty of Physics, University of Science, Vietnam National University, Hanoi, Vietnam
e-mail: luanpt@hus.edu.vn